

MECHANICAL ANALYSIS OF 2D-BRAZED JOINT USING A NEW HYBRID “MAX-FEM” MODEL

A. IFIS^(a), F. Bilteryst^(b), M. Nouari^(c)

(a) Laboratoire d’Énergétique et de Mécanique Théorique et Appliquée, LEMTA CNRS-UMR 7563, GIP-InSIC, 27 rue d’Helleuille, 88100, Saint Dié des Vosges, France

(b) Laboratoire d’Énergétique et de Mécanique Théorique et Appliquée, LEMTA CNRS-UMR 7563, GIP-InSIC, 27 rue d’Helleuille, 88100, Saint Dié des Vosges, France

(c) Laboratoire d’Énergétique et de Mécanique Théorique et Appliquée, LEMTA CNRS-UMR 7563, GIP-InSIC, 27 rue d’Helleuille, 88100, Saint Dié des Vosges, France

^(a)abderrazzaq.ifis@gmail.com ^(b)francois.bilteryst@insic.fr ^(c)mohammed.nouari@insic.fr

ABSTRACT

This work deals with the performance of a new approach combining the numerical eXtended Finite Elements Method ‘X-FEM’ and the analytical method of Matched Asymptotic Expansions ‘MAE’. The proposed new “MAX-FEM” model is well adapted for studying and modeling the mechanical behavior of mediums containing singularities such as thin layers or adhesive joints without any required mesh refinement in their vicinity. The methodology consists of the construction of enrichment parameters with the ‘MAE’ technique and their integration into the ‘XFEM’ formulation. Correction matrix of stiffness is then defined and integrated in the FEM computation algorithm. To describe the mechanical behavior of a proposed structure with 2D brazed joints, the “MAX-FEM” hybrid model has been implemented as an UEL subroutine under Abaqus implicit. Compared with the classical FE method, the obtained results in terms of stress field, strains and displacements show a good accuracy without any required mesh refinement.

Keywords: hybrid technique, thin layers, Matched Asymptotic Expansions, X-FEM, correction matrix, UEL ‘MAX-FEM’ subroutine.

1. INTRODUCTION

During the last decade, several methods have been introduced for modelling singular problems such as thin layers, adhesive joints, coating, etc.. Analytical approaches based on asymptotic assumptions such as Matched Asymptotic Expansions (MAE) give at two different-scales an approximation of the main solution in structures containing singularities (M. Van Dyke, 1975; P. Schmidt, 2008). As shown by the work of Leguillon and Abdelmoula (2000), the MAE method has been used to analyse brazed joints in order to describe the crack propagation process at the interface between the joint and the bonded substrates. However the difficulty of the numerical implementation of this method makes its use very complicated and limited to some simple cases.

In the other side, the numerical methods headed by the Finite Element Method (FEM) struggle with singular problems, where a mesh refinement is required

in order to take into account singularities. Besides, in order to overcome this limitation, particular numerical methods have been introduced to deal with this difficulty. These methods allow to give a multi-scale analysis in discontinuous mediums as assembly structures, welded mediums, etc.. Two possibilities are given by these approaches: the first procedure consists in making a local analysis and then project the information about the singularity behaviour at the large scale. The homogenization and the Arlequin methods, described by (T.I. Zohdi, J.T. Oden and G.J. Rodin, 1996) and (P.T. Bauman and H. Ben Dhia, 2008) respectively, are based on this principle and are used in several works, especially to analyse composites materials. The second procedure consists in defining a correction of the classical FE method. The information about the singularity is then stored in an added part called “enrichment”. Thereby, the local analysis is not required. X-FEM (N. Moes, J. Dolbow and T. Belytschko, 1999; H. Bayesteh and S. Mohammadi, 2011) and G-FEM (I. Babuska, U. Banerjee and J. Osborn, 2004) are two partition of unity (PUM) (I. Babuska and J.M Melenk, 1999) methods that are used in several works in order to solve various types of problems especially crack problems.

2. STATE OF THE ART: METHODS USED FOR SINGULAR PROBLEMS

2.1. X-FEM approach:

Problems with singularities have been firstly treated using FE method by updating the mesh ‘topology’ in order to match the geometry of the singularity. However, the introduction of X-FEM circumvents this problem by enriching a standard approximation with special additional functions. The form of the enriched approximation follows the partition of unity. The geometry of the singularity is then involved by updating the enrichment scheme; no remeshing of the domain is required. The only interaction between the mesh and the geometry of the singularity involves the construction of the enriched basis functions. The classical X-FEM formulation is given by:

$$\mathbf{u}(\mathbf{x}) = \sum_i^N N_i(\mathbf{x}) \mathbf{u}_i + \sum_k^{N_{enr}} N_k(\mathbf{x}) \psi_k(\mathbf{x}) \mathbf{b}_k \quad (1)$$

Where N_{enr} is the enrichment terms number, $\mathbf{u}(\mathbf{x})$ the approximated function, $N_i(\mathbf{x})$ the standard FEM functions for node i , \mathbf{u}_i the unknown of the standard FEM part at node i , ψ_k the enrichment function and \mathbf{b}_k the enrichment parameter.

2.2. MAE approach:

MAE approach has been firstly used for fluid mechanics (M. Van Dyke, 1975). It shows its efficiency in treating perturbed problems and boundary layers. This method based on asymptotic assumptions has been applied for adhesive joint problems as illustrated in Figure 1.

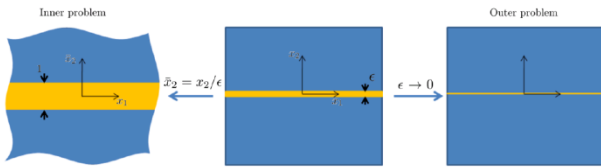


Figure 1. Two-scales partition of 'Matched Asymptotic Expansions' approach.

It consists in solving problems at two different scales (Figure 1) by introducing two different asymptotic expansions, the outer (Equation 2) and the inner (Equation 3) expansions.

$$\mathbf{u}^\pm(x_1, x_2) = \mathbf{u}^{0\pm}(x_1, x_2) + \varepsilon \mathbf{u}^{1\pm}(x_1, x_2) + \dots \quad (2)$$

$$\mathbf{v}^\pm(x_1, \bar{x}_2) = \mathbf{v}^{0\pm}(x_1, \bar{x}_2) + \varepsilon \mathbf{v}^{1\pm}(x_1, \bar{x}_2) + \dots \quad (3)$$

With \bar{x}_2 is the stretched variable $\bar{x}_2 = x_2 / \varepsilon$ and $(\cdot)^\pm$ denotes the displacement values at the both sides of the interface ($\bar{x}_2 = x_2 = 0$).

Each expansion is constituted of two main parts: the leading terms \mathbf{u}^0 and \mathbf{v}^0 which are the classical solutions obtained by finite element method while the second part is considered as a correction given by a perturbed terms $\varepsilon \mathbf{u}^1$ and $\varepsilon \mathbf{v}^1$ depending on ε ; the characteristic thickness of the brazed joint.

In the works of (D. Leguillon and R. Abdelmoulab, 2000; D.H. Nguyen et al., 2008), the MAE has been used to compute the jumps expressions of displacement field across the interface of discontinuity defined by the outer domain. This algorithm is based on simultaneous resolution of classical equations of the model (equilibrium equations, constitutive laws, continuity conditions) for each order, and a matching process

(Equation 4) for both expansions at their respective limits (i.e. $x_2 \rightarrow 0$) for the outer expansion, and $\bar{x}_2 \rightarrow \pm\infty$ for the inner expansion).

$$\begin{cases} \lim_{\bar{x}_2 \rightarrow \pm\infty} (\mathbf{v}^{0\pm}(x_1, \bar{x}_2) - \mathbf{u}^{0\pm}(x_1, 0)) = 0 \\ \lim_{\bar{x}_2 \rightarrow \pm\infty} \left(\mathbf{v}^{1\pm}(x_1, \bar{x}_2) - \bar{x}_2 \frac{\partial \mathbf{u}^{0\pm}}{\partial \bar{x}_2}(x_1, 0) - \mathbf{u}^{1\pm}(x_1, 0) \right) = 0 \\ \dots \end{cases} \quad (4)$$

Using this algorithm, the jump \mathbf{u} of displacement (D. Leguillon and R. Abdelmoulab, 2000; D.H. Nguyen et al., 2008) is computed and expressed by:

$$\mathbf{u} = \begin{cases} \varepsilon [u_1^{+}(x_1, 0) - u_1^{-}(x_1, 0)] = \varepsilon \frac{\mu_1 - \mu_2}{\mu_2} [u_{2,1}^{0-}(x_1, 0) + u_{1,2}^{0-}(x_1, 0)] + \\ \varepsilon \frac{\mu_1 - \mu_2}{\mu_2} [u_{2,1}^{0+}(x_1, 0) + u_{1,2}^{0+}(x_1, 0)] \\ \varepsilon [u_2^{+}(x_1, 0) - u_2^{-}(x_1, 0)] = \varepsilon \left[\frac{\lambda_1 - \lambda_2}{\lambda_2 + 2\mu_2} u_{1,1}^{0-}(x_1, 0) + \left[\frac{\lambda_1 + 2\mu_1}{\lambda_2 + 2\mu_2} - 1 \right] u_{2,2}^{0-}(x_1, 0) \right] + \\ \varepsilon \left[\frac{\lambda_1 - \lambda_2}{\lambda_2 + 2\mu_2} u_{1,1}^{0+}(x_1, 0) + \left[\frac{\lambda_1 + 2\mu_1}{\lambda_2 + 2\mu_2} - 1 \right] u_{2,2}^{0+}(x_1, 0) \right] \end{cases} \quad (5)$$

As it will be presented in the next section, this value has been used in the setup of the MAX-FEM model.

2.3. Proposed hybrid MAX-FEM Model

In this work, the hybrid MAX-FEM model has been introduced for the thin layers modelling to release mechanical analysis of a 2D-brazed joint. The MAX-FEM model is a Partition of Unity Method (PUM) where the main solution is formulated using two main parts: a classical FEM discretization and the enrichment terms. The proposed PUM formulation exploits the Matched Asymptotic Expansions (MAE) in the definition of the enrichment parameters. This procedure links the two main parts of the PUM formulation to give a corrected form of the standard FEM where correction matrix is introduced to compute the stiffness matrix.

3. MAX-FEM SETUP

3.1. MAX-FEM Principle

By analysing the shapes of the X-FEM and MAE approaches, it is notable that these two methods share the common subdivision of the unknown solution at two different parts: the classical solution and the correction terms (Figure 2). Thereby the MAX-FEM model feats the similarity between the two methods to define a new procedure describing the brazed joint behaviour. In fact, the joint is assimilated to a discontinuity interface which creates a jump of displacement field. The new configuration containing the introduced singularity is

described using a specific MAX-FEM formulation while the enrichment parameters are defined using the jumps computed by the MAE approach (Equation 5).

$$u(x) = \sum_i^N N_i(x) u_i + \sum_k^{N_{enr}} N_k(x) \psi_k(x) b_k \quad u(x) = u^0(x) + \varepsilon u^1(x)$$

Non-perturbed term correction term

Figure 2. Identification of leading and correction terms using MAX-FEM model.

3.2. Problem position

The main purpose here is the setup of the MAX-FEM model for a 2D-brazed joint under mechanical loading (see Figure 3). The adhesive joint and substrates are considered as elastic domains.

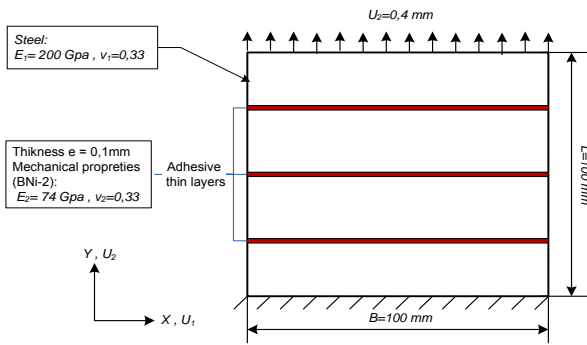


Figure 3. 2D brazed joint under mechanical loading

3.3. MAX-FEM formulation

The MAE outer expansion (Equation 2) crushes the thin layer. The latter is turned to an interface of discontinuity ($\varepsilon \rightarrow 0$) which completely crosses the width of the assembly (see Figure 1). As a result, the problem is assimilated to the strong discontinuity problem with presence of displacement jump across the interface. Herein, the MAX-FEM will consider the formulation (Equation 1) and adapts it to the considered application. In this context, the formulation proposed in equation (6) uses the same strategy as the outer expansion of MAE while keeping the basic shape of X-FEM:

$$\mathbf{u}(\mathbf{x}) = \sum_i^N N_i(\mathbf{x}) \mathbf{u}_i^0 + \sum_k^{N_{enr}} N_k(\mathbf{x}) H(\mathbf{x}_k) \mathbf{b}_k \quad (6)$$

Where \mathbf{b}_k and are the enrichment parameters which must be defined and H is the Heaviside function

defined in the point $\mathbf{x} \begin{pmatrix} x_1 \\ x_2 \end{pmatrix}$ by:

$$H(\mathbf{x}) = \begin{cases} -1 & \text{if } x_2 < 0 \\ 1 & \text{if } x_2 \geq 0 \end{cases}$$

Instead of using nodal values of the global field \mathbf{u}_i as used in formulation (Equation 1) and in the work of Nguyen et al. (2008), this approximation (Equation 6) integrates the continuous solution \mathbf{u}^0 .

The similarity between the outer expansion (Equation 2) and formulation (Equation 6) is employed to identify the enrichment parameters $\mathbf{b}_k \begin{pmatrix} a_k \\ b_k \end{pmatrix}$. The algorithm of identification is illustrated for linear structural element containing the joint position (Figure 4):

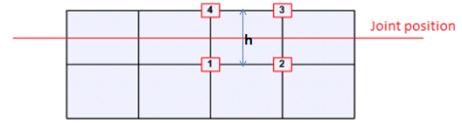


Figure 5. Linear structural enriched element containing the joint position

Equations (6) and (2) are used to compute the nodal values of the global fields (Equation 7) and (Equation 8) as follow:

Firstly, by using the formulation (Equation 6):

$$\begin{cases} u_1(\mathbf{x}_1) = u_1^0(\mathbf{x}_1) - a_1 \\ u_1(\mathbf{x}_2) = u_1^0(\mathbf{x}_2) - a_2 \\ u_1(\mathbf{x}_3) = u_1^0(\mathbf{x}_3) + a_3 \\ u_1(\mathbf{x}_4) = u_1^0(\mathbf{x}_4) + a_4 \end{cases} \quad \begin{cases} u_2(\mathbf{x}_1) = u_2^0(\mathbf{x}_1) - b_1 \\ u_2(\mathbf{x}_2) = u_2^0(\mathbf{x}_2) - b_2 \\ u_2(\mathbf{x}_3) = u_2^0(\mathbf{x}_3) + b_3 \\ u_2(\mathbf{x}_4) = u_2^0(\mathbf{x}_4) + b_4 \end{cases} \quad (7)$$

And secondly, by using MAE outer expansion (Equation 2):

$$\begin{cases} u_1(\mathbf{x}_1) = u_1^0(\mathbf{x}_1) + \varepsilon u_1^1(\mathbf{x}_1) \\ u_1(\mathbf{x}_2) = u_1^0(\mathbf{x}_2) + \varepsilon u_1^1(\mathbf{x}_2) \\ u_1(\mathbf{x}_3) = u_1^0(\mathbf{x}_3) + \varepsilon u_1^1(\mathbf{x}_3) \\ u_1(\mathbf{x}_4) = u_1^0(\mathbf{x}_4) + \varepsilon u_1^1(\mathbf{x}_4) \end{cases} \quad \begin{cases} u_2(\mathbf{x}_1) = u_2^0(\mathbf{x}_1) + \varepsilon u_2^1(\mathbf{x}_1) \\ u_2(\mathbf{x}_2) = u_2^0(\mathbf{x}_2) + \varepsilon u_2^1(\mathbf{x}_2) \\ u_2(\mathbf{x}_3) = u_2^0(\mathbf{x}_3) + \varepsilon u_2^1(\mathbf{x}_3) \\ u_2(\mathbf{x}_4) = u_2^0(\mathbf{x}_4) + \varepsilon u_2^1(\mathbf{x}_4) \end{cases} \quad (8)$$

Then, the displacement difference between two nodes located on the same ridge and crossing the joint position is computed with the two approximations (Equation 7) and (Equation 8) as follow.

Firstly, by using the formulation (Equation 7):

$$\begin{cases} u_1(\mathbf{x}_4) - u_1(\mathbf{x}_1) = u_1^0(\mathbf{x}_4) - u_1^0(\mathbf{x}_1) + a_4 + a_1 \\ u_1(\mathbf{x}_3) - u_1(\mathbf{x}_2) = u_1^0(\mathbf{x}_3) - u_1^0(\mathbf{x}_2) + a_3 + a_2 \end{cases} \quad \begin{cases} u_2(\mathbf{x}_4) - u_2(\mathbf{x}_1) = u_2^0(\mathbf{x}_4) - u_2^0(\mathbf{x}_1) + b_4 + b_1 \\ u_2(\mathbf{x}_3) - u_2(\mathbf{x}_2) = u_2^0(\mathbf{x}_3) - u_2^0(\mathbf{x}_2) + b_3 + b_2 \end{cases} \quad (9)$$

Secondly, by using MAE outer expansion (Equation 8):

$$\begin{cases} u_1(\mathbf{x}_4) - u_1(\mathbf{x}_1) = u_1^0(\mathbf{x}_4) - u_1^0(\mathbf{x}_1) + \varepsilon(u_1^1(\mathbf{x}_4) - u_1^1(\mathbf{x}_1)) \\ u_1(\mathbf{x}_3) - u_1(\mathbf{x}_2) = u_1^0(\mathbf{x}_3) - u_1^0(\mathbf{x}_2) + \varepsilon(u_1^1(\mathbf{x}_3) - u_1^1(\mathbf{x}_2)) \\ u_2(\mathbf{x}_4) - u_2(\mathbf{x}_1) = u_2^0(\mathbf{x}_4) - u_2^0(\mathbf{x}_1) + \varepsilon(u_2^1(\mathbf{x}_4) - u_2^1(\mathbf{x}_1)) \\ u_2(\mathbf{x}_3) - u_2(\mathbf{x}_2) = u_2^0(\mathbf{x}_3) - u_2^0(\mathbf{x}_2) + \varepsilon(u_2^1(\mathbf{x}_3) - u_2^1(\mathbf{x}_2)) \end{cases} \quad (10)$$

The equality between Equations (9) and (10) gives the conditions that the enrichment parameters have to satisfy:

$$\begin{cases} a_4 + a_1 = \varepsilon(u_1^1(\mathbf{x}_4) - u_1^1(\mathbf{x}_1)) \\ a_3 + a_2 = \varepsilon(u_1^1(\mathbf{x}_3) - u_1^1(\mathbf{x}_2)) \\ b_4 + b_1 = \varepsilon(u_2^1(\mathbf{x}_4) - u_2^1(\mathbf{x}_1)) \\ b_3 + b_2 = \varepsilon(u_2^1(\mathbf{x}_3) - u_2^1(\mathbf{x}_2)) \end{cases} \quad (11)$$

To compute these parameters values, it is not necessary to have an explicit expression of the perturbed term \mathbf{u}^1 in each node. In fact, by using the MAE algorithm introduced in works (D. Leguillona and R. Abdelmoulab, 2000; D.H. Nguyen et al., 2008) the term $\varepsilon(\mathbf{u}^1(\mathbf{x}_4) - \mathbf{u}^1(\mathbf{x}_1))$ for nodes 1 and 4 (respectively $\varepsilon(\mathbf{u}^1(\mathbf{x}_3) - \mathbf{u}^1(\mathbf{x}_2))$ for nodes 2 and 3) are approximated to $\varepsilon(1-h) \mathbf{u}^1(x_1^{1-4}, 0)$ and $\varepsilon(1-h) \mathbf{u}^1(x_1^{2-3}, 0)$, respectively. h is the height of the enriched element while $\mathbf{u}^1(x_1^{1-4}, 0)$ (respectively $\mathbf{u}^1(x_1^{2-3}, 0)$) denotes the displacement jump crossing the interface in the common abscissa between nodes 1 and 4 (respectively 2 and 3).

Taking into account the previous approximation, the expression proposed for the parameters \mathbf{b}_k is given below:

$$\mathbf{b}_k = \begin{cases} \frac{\varepsilon}{2} (1-h) \mathbf{u}^1(x_1^{1-4}, 0) & \text{for } k = 1, 4 \\ \frac{\varepsilon}{2} (1-h) \mathbf{u}^1(x_1^{2-3}, 0) & \text{for } k = 2, 3 \end{cases} \quad (12)$$

3.4. Stiffness matrix

The expression (Equation 5) shows a linear dependence between the jump and the leading derivative terms. From this dependence rises a transfer matrix between the jump and the unperturbed strain vector:

$$\mathbf{u}^1 = \begin{Bmatrix} u_1^1 \\ u_2^1 \end{Bmatrix} = \begin{bmatrix} 0 & 0 & A \\ B & S & 0 \end{bmatrix} \begin{Bmatrix} u_{1,1}^0(x_1, 0) \\ u_{2,2}^0(x_1, 0) \\ u_{1,2}^0(x_1, 0) + u_{1,2}^0(x_1, 0) \end{Bmatrix} = [\mathbf{C}] \{\varepsilon^0\} \quad (13)$$

$\{\varepsilon^0\}$ is the leading strain vector, $[\mathbf{C}] = \begin{bmatrix} 0 & 0 & A \\ B & S & 0 \end{bmatrix}$,

$$A = \frac{\mu_1 - \mu_2}{\mu_2}, \quad B = \frac{\lambda - \lambda_2}{\lambda_2 + 2\mu_2} \quad \text{and} \quad S = \frac{\lambda + 2\mu}{\lambda_2 + 2\mu_2} - 1.$$

By integrating this result in the enrichment parameters expression, the latter are linked to the leading term nodal values as shown in (Equation 14).

$$\mathbf{b}_k = \begin{cases} \frac{\varepsilon}{2} (1-h) [\mathbf{C}] [\mathbf{B}] (x_1^{1-4}, 0) \{u^0\} & \text{for } k = 1, 4 \\ \frac{\varepsilon}{2} (1-h) [\mathbf{C}] [\mathbf{B}] (x_1^{2-3}, 0) \{u^0\} & \text{for } k = 2, 3 \end{cases} \quad (14)$$

$[\mathbf{C}]$ is the enrichment matrix defined in (Equation 13) and $[\mathbf{B}]$ is the strain matrix linking the strain vector to the nodal values of the leading term.

The expression (Equation 14) is injected in the X-FEM formulation (Equation 6) creating then a transfer matrix between the global nodal displacement values $\{u\}$ and the leading term one $\{u^0\}$:

$$\{u\} = \left([\mathbf{I}]_{8,8} + \frac{1}{2} [\mathbf{H}] [\mathbf{C}] [\mathbf{B}] (x_1, 0) \right) \{u^0\} \quad (15)$$

$[\mathbf{I}]_{8,8}$ is the identity matrix and $[\mathbf{H}]$ is called ‘‘Heaviside matrix’’ and expressed below:

$$[\mathbf{H}] = \begin{bmatrix} H(\mathbf{x}_1) & 0 & H(\mathbf{x}_2) & 0 & H(\mathbf{x}_3) & 0 & H(\mathbf{x}_4) & 0 \\ 0 & H(\mathbf{x}_1) & 0 & H(\mathbf{x}_2) & 0 & H(\mathbf{x}_3) & 0 & H(\mathbf{x}_4) \end{bmatrix}$$

By considering that the global problem and the leading outer one are assumed under the same exterior loading ($\{F\} = \{F^0\}$), the global stiffness matrix $[\mathbf{K}]$ is linked to the one of the leading problem $[\mathbf{K}^0]$ as follow:

$$[\mathbf{K}] = \int_{\Omega} [\mathbf{B}] [\mathbf{D}] [\mathbf{B}] \left([\mathbf{I}]_{8,8} + \frac{1}{2} [\mathbf{H}] [\mathbf{C}] [\mathbf{B}] (x_1, 0) \right)^{-1} d\Omega \quad (16)$$

Consequently, the global stiffness matrix can be defined as a correction of the standard FEM stiffness matrix using a ‘‘correction matrix’’ $[\mathbf{CM}]$ defined by:

$$[\mathbf{CM}] = \left([\mathbf{I}]_{s,s} + \frac{1}{2} [\mathbf{H}] [\mathbf{C}] [\mathbf{B}] (x_1, 0) \right)^{-1} \quad (17)$$

Finally, the linear system to consider is:

$$[\mathbf{K}] \{u\} = \{F\} \quad (18)$$

The enrichment parameters \mathbf{b}_k and the leading term \mathbf{u}^0 of the finite elements formulation (Equation 6) do not appear explicitly in the final system (Equation 18). This is due to the MAE results which reveal a linear dependence linking the enrichment parameters to the leading term derivatives. Also, the continuity of the finite elements formulation (Equation 6) allows to define a correction matrix $[\mathbf{CM}]$ (Equation 17) and to link the global stiffness matrix $[\mathbf{K}]$ to the standard one.

The computation of the leading term \mathbf{u}^0 and the enrichment parameters is then not needed, and the global displacement field \mathbf{u} is directly computed by numerical resolution of the system (Equation 18). It can be noted that only the correction matrix $[\mathbf{CM}]$ is computed and then injected in a standard FEM program.

The obtained solution covers the outer domains. This means that only the influence of the thin layer on the global structure is characterized. In this work, the local analysis of the thin layer is not considered. However, if necessary, the model can take into account the complex behavior in the vicinity of the joint, including crack, delamination or other nonlinear aspects for example. This can be possible by resolving the inner problem (Equation 3) of the MAE. Following this approach, the local analysis is restricted in the enriched elements which are expanded to zoom on the joint and the contact interfaces. The resolution of the inner problem can be performed by using the existing methods (FEM, X-FEM, etc.).

4. NUMERICAL IMPLEMENTATION OF MAX-FEM MODEL

This section provides a validation study for the proposed MAX-FEM hybrid model. The obtained results are compared to those given by the standard FEM by meshing finely the thin layer. In this work, ABAQUS code is used to implement the model using an UEL subroutine. The same code is also used to compute the reference solution (FEM) for 2D-brazed joint in figure 3

4.1. Numerical implementation

The model developed here has been implemented in ABAQUS as a user element using the UEL subroutine. The procedure of the development of this subroutine is based on a previous work introduced by Giner et al. (2009). The model starts from a

combination of X-FEM and MAE, and will give as a final result the corrected form of standard FEM. This correction is presented by the matrix $[\mathbf{CM}]$ (Equation 17) which stores the required information for the joint behavior. As a result, the structure of the program (Figure 4) will be constituted by the standard FEM while the correction matrix will be computed in an internal subroutine depending on the considered application.

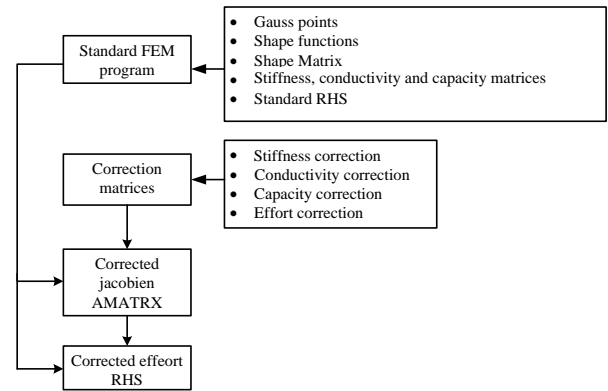


Figure 5. Algorithm structure of the implemented UEL “MAX-FEM” subroutine

The results given in the setup of the model are implemented in the UEL “MAX-FEM” subroutine following the structure presented in Figure 6. The correction matrix $[\mathbf{CM}]$ (Equation 17) and the corrected stiffness matrix (Equation 16) are computed for the 2D-brazed joint presented in Figure 3.

The computation is limited to 2D plane stress state. Thereby, the enrichment matrix $[\mathbf{C}]$ (Equation 13) needed for the computation of the correction matrix $[\mathbf{CM}]$ (Equation 26) is written as:

$$[\mathbf{C}] = \varepsilon \left(\frac{E_1}{E_2} - 1 \right) \begin{bmatrix} 0 & 0 & 1 \\ \nu & 1 & 0 \end{bmatrix} \quad (19)$$

By resolving the system (Equation 18), the displacement field is obtained. Then, other mechanical fields are deduced. The results given by the UEL “MAX-FEM” subroutine are compared to ones obtained by standard FEM under the same code. The considered mesh, displacement, stress, strain and error are presented for the two methods.

(i) Mesh

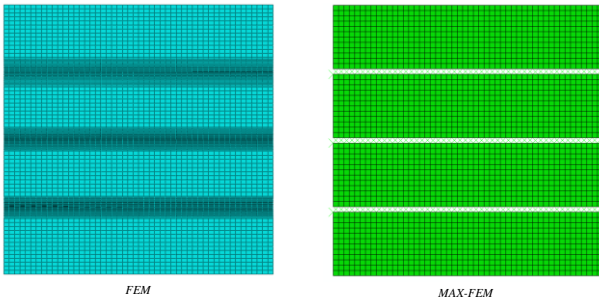


Figure 6. Overview of the classical FEM discretization and the MAX-FEM meshing

User elements are not represented by ABAQUS post-processor. However, in order to reach this aim, a post-processing subroutine should be required. This will be performed in forthcoming developments.

The comparison between the two mesh strategies is summarized in Table 1:

Table 1. FEM and MAX-FEM mesh data

	FEM	MAX-FEM	Ratio (FEM/MAX-FEM)
Nodes number	7242	2652	2,73
Elements number	7052	2550	2,76
Minimum element size	0,1 mm	2 mm	20

From Table 1, it can be noted that the model presents an important mesh optimization. This should be more notable in forthcoming transient analyses where the time increment for such computations depends on the size of elements.

(ii) Stress

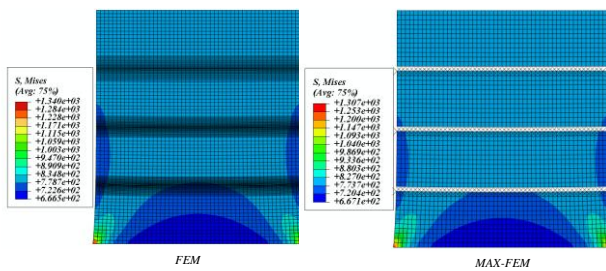


Figure 7. FEM and MAX-FEM stress distributions

(iii) Displacement

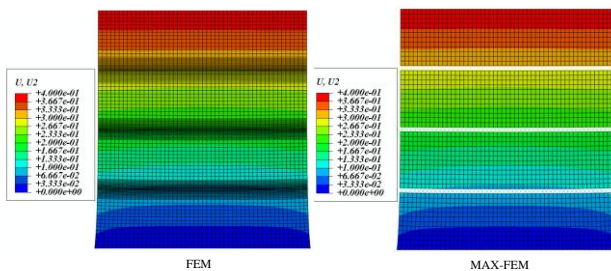


Figure 8. FEM and MAX-FEM displacements

By analyzing these results, it can be noted that the model reproduces the outer displacements and stress fields given by the FEM method. In order to give an accurate comparison, a plot of the displacements in the section $x = 20 \text{ mm}$ are presented in Figure 13:

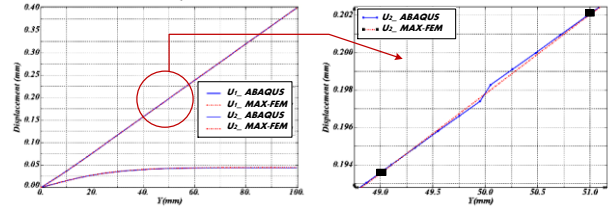


Figure 9. FEM and MAX-FEM displacements in the section $x = 20 \text{ mm}$

Figure 8 shows that the curve given by the model fits the one obtained by standard FEM from the first enriched node. Consequently, a single MAX-FEM element reproduces the same solution given by several FEM elements. The line linking the two enriched nodes is a linear interpolation and does not present the solution in the vicinity of the joint. The latter can be obtained by the resolution of the inner problem of MAE.

To analyze the accuracy of the model, three error expressions are computed taking the FEM solution as reference:

- Relative error: $err_{relative} = \frac{|u_{FEM}^i - u_{MAX-FEM}^i|}{u_{FEM}^i}$
- Maximum error: $err_{max} = \max(|u_{FEM}^i - u_{MAX-FEM}^i|)$
- Norm L^2 : $\|err\| = \sqrt{\sum (u_{FEM}^i - u_{MAX-FEM}^i)^2}$

These expressions are used to estimate the error into the section $x = 20 \text{ mm}$ by using the previous results of Figure 8

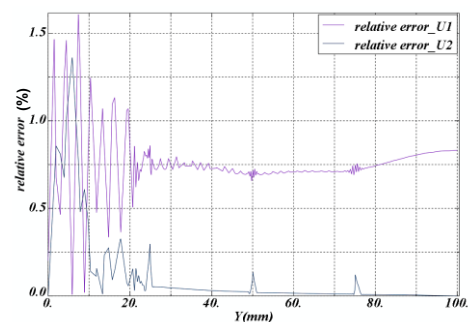


Figure 10. Relative error in the section $x = 20 \text{ mm}$

Table 2. error approximation

	$\max(err_{relative})$	err_{max}	$\ err\ $
U1	1,6 %	0,0039	1,339 10-7
U2	1,36 %	0,00128	1,295 10-7

By analyzing these error approximations, it becomes trivial that the hybrid model presents accurate results without meshing the thin layer. However, the

accuracy of the model depends on several parameters and the model can have some limitations and critical points.

Among these limitations, there are boundary problems which affect the results accuracy near to boards. These problems are especially due to the MAE method. The rules used to link the outer and inner solutions still available in an infinite inner domain. However, in the boards, the solution has to satisfy the boundary conditions. The enrichment strategy used in this work cannot then reproduce the solution in the vicinity of boards.

In addition to board problems, other parameters may affect the model accuracy. The three points below are the most important:

1. The ratio h/e linking the element height and the joint thickness. Actually, more this ratio is smaller; more the results highlight a good accuracy.
2. The number of enriched elements: in this work, a single element is enriched in the joint thickness direction. However, it is trivial that increasing that number will increase the model accuracy. Besides, a new enrichment strategy has to be developed.

5. CONCLUSION

The hybrid model introduced in this work combines the MAE technique which is used to define the enrichment parameters and the X-FEM formulation. This new approach called 'MAX-FEM' model has been established and used to solve the mechanical singular problem of two-dimensional brazed joints. The 'MAX-FEM' approach leads to a corrected form of standard FEM where a correction matrix is used to compute the main solution in the whole structure.

Once set up, the model has been implemented under ABAQUS code using the UEL subroutine. The results given by the model are compared to those obtained using standard FEM for the 2D- brazed joint. From this application, it is notable that "MAX-FEM" model provides accurate results in terms of displacement and temperature fields without any required mesh refinement in the vicinity of the thin layer.

However, the model has its limitations near to boards where the proposed enrichment is not available. New enrichment strategies have to be developed in future work to deal with this limitation. Also, even if it is not developed here, the model can take into account other behaviors of the joint such as damage, cracks and delamination. These behaviors have to be considered in the computation of jumps using MAE approach. Besides, if it is necessary, the local behavior of the joint can be described by the resolution of the inner problem. Thereby the analysis can be developed in two scales instead of the global analysis presented in this work. Finally, it can be said that the model needs to be

enhanced and generalized to be used for more complicated applications.

REFERENCES

- I. Babuska, J.M Melenk, *The partition of unity finite element method*, Int. J.Numer.Meth.Engrg.40 (1997) 727-758
- I. Babuska, U. Banerjee, J. Osborn, *Generalized finite element methods: Main ideas, results, and perspective*, Int. J. Comput. Methods 1 (1) (2004) 1-37
- P.T. Bauman, H. Ben Dhia, N. Elkhodja, J.T. Oden, S. Prudhomme, *On the application of the Arlequin method to the coupling of particle and continuum models*, Comput. Mech., 42 (2008) 511–530.
- H. Bayesteh, S. Mohammadi, *XFEM fracture analysis of shells: The effect of crack tip enrichments*, Computational Materials Science, 50 (2011) 2793–2813
- Giner E, Sukumar N, Tarancon JE, Fuenmayor FJ. *An Abaqus implementation of the extended finite element method*. Eng Fract Mech., 76 (2009) 347-368.
- D. Leguillona, R. Abdelmoulab, *Mode III near and far fields for a crack lying in or along a joint*, International Journal of Solids and Structures, 37 (2000) 2651-2672
- N. Moes, J. Dolbow, T. Belytschko, *A finite element method for crack growth without remeshing*, Int. J. Numer. Meth. Engrg. 46 (1999) 131–150.
- D. H. Nguyen, F. Bilteryst, M. Lazard, P. Lamesle, G. Dour, *Coupling of the eXtended Finite Element Method and the matched asymptotic development in the modelling of brazed assembly*, International Journal of Material Forming, 1, 2008, pp. 1119-1122
- P. Schmidt, *Modeling of adhesively bonded joints by an asymptotic method*, International Journal of Engineering Science, 46 (2008) 1291–1324
- M. Van Dyke, *perturbation methods in fluid Mechanics* (1975)
- T.I. Zohdi, J.T. Oden, G.J. Rodin, *Hierarchical modeling of heterogeneous bodies*. Computer Methods in Applied Mechanics and Engineering, 138 (1996) 273-298,